Mechanism of the Carotenoid-to-Bacteriochlorophyll Energy Transfer via the S_1 State in the LH2 Complexes from Purple Bacteria

Jian-Ping Zhang,[†] Ritsuko Fujii,[†] Pu Qian,[†] Toru Inaba,[†] Tadashi Mizoguchi,[†] Yasushi Koyama,*[,†] Kengo Onaka,[‡] and Yasutaka Watanabe[‡]

Departments of Chemistry and Physics, Faculty of Science, Kwansei Gakuin University, Uegahara, Nishinomiya 662-8501, Japan

Hiroyoshi Nagae

Kobe City University of Foreign Studies, Gakuen Higashimachi, Nishiku, Kobe 651-2187, Japan

Received: November 9, 1999; In Final Form: January 27, 2000

This investigation was motivated by a desire to get a deeper insight into the mechanism of carotenoiod-to-bacteriochlorophyll (Car-to-BChl) energy transfer proceeding via the carotenoid S_1 state. (Here, we call the $2A_g^-$ and $1B_u^+$ states "the S_1 and S_2 states" according to the notation presently accepted.) To systematically examine the effect of the conjugation length of carotenoid on the rate and efficiency of the Car(S_1)-to-BChl-(Q_y) energy transfer, we performed the following experiments. (1) Subpicosecond time-resolved absorption spectroscopy was employed to measure the S_1-state lifetimes of lycopene (number of conjugated C═C bonds, $n = 11$), spheroidene ($n = 10$), and neurosporene ($n = 9$), both free in *n*-hexane and bound to the LH2 complexes from *Rhodospirillum molischianum* (*Rs. molischianum*), *Rhodobactor sphaeroides* (*Rb. sphaeroides*) 2.4.1, and *Rb. sphaeroides* G1C, respectively. The lifetime of each free (bound) carotenoid was determined to be 4.7(3.4) ps for lycopene, 9.3(1.7) ps for spheroidene, and 21.2(1.3) ps for neurosporene. It was found that the rate and the efficiency of the Car(S_1)-to-BChl(Q_y) energy transfer increase systematically when the number of conjugated C═C bonds decreases. (2) High-sensitivity steady-state fluorescence spectroscopy was used to measure the spectra of dual emission from the S_2 and S_1 states for the above carotenoids dissolved in *n*-hexane. The fluorescence data, combined with the above kinetic data, allowed us to evaluate the magnitudes of the transition-dipole moments associated with the Car(S_1) emission. It was found that the S_1 emissions of the above carotenoids carry noticeably large oscillator strengths (transition-dipole moments). In the case of the LH2 complex from *Rs. molischianum*, whose structural information is now available, the time constant of the Car(S_1)-to-BChl(Q_y) energy transfer (18.6 ps), which was predicted on the basis of a Car(S_2)-to-BChl-(Q_y) full Coulombic coupling scaled by the ratio of the S_1 vs S_2 transition dipole moments, was in good agreement with the one spectroscopically determined (12.3 ps). The oscillator strength associated with the Car(S_1) emission was discussed in terms of the state mixing between the carotenoid S_2 and S_1 states.

1. Introduction

In the antenna complexes of photosynthetic bacteria, *all-trans*-carotenoid (Car) realizes the light-harvesting function through its strong absorption around 500 nm, and the subsequent singlet energy transfer to bacteriochlorophyll (BChl).[1,2] Recently, this issue has attracted intensive research interests largely owing to the success in determining the structures of the LH2 complexes from purple bacteria, i.e., *Rhodopseudomonas acidophila*[3] (*Rps. acidophila*) and *Rhodospirillum molischianum*[4] (*Rs. molischianum*). Both experimental and theoretical efforts have been directed to the understanding of the mechanism of Car-to-BChl energy transfer.[5−12]

It is generally accepted that two low-lying singlet excited states, S_2 and S_1, of carotenoid are involved in the light-harvesting processes. In analogy to *all-trans*-polyenes belonging to the C_{2h} point group, $1B_u^+$, $2A_g^-$, and the ground state, $1A_g^-$, of carotenoid are also denoted as S_2, S_1, and S_0, respectively. (The above notation of the singlet states needs to be changed, since another dark state, $1B_u^-$, has recently been discovered between the $1B_u^+$ and $2A_g^-$ states.[13,14] However, in this paper, we will continue, to avoid confusion, to use the above numbering of the singlet states which is now well accepted.) The $S_2(1B_u^+)$ state, which is responsible for the aforementioned visible absorption, is characterized by the very low fluorescence quantum yield ($<10^{-4}$, in organic solvents),[15,16] and its short lifetime which is on the time scale of subpicoseconds.[5,17,18] Although the transition from the $S_0(1A_g^-)$ state is optically forbidden, the $S_1(2A_g^-)$ state can be efficiently populated via the rapid $S_2 \rightarrow S_1$ internal conversion; this state has a lifetime of a few to a few tens of picoseconds depending on the number of conjugated C═C bonds.[2] The S_1 state was historically proposed to be kinetically favorable in mediating the Car-to-BChl energy transfer. Furthermore, due to its optically forbidden nature (vanishing transition-dipole moment), the S_1 state was once proposed to transfer the singlet energy to the Q_y state of BChl via the electron exchange-type interaction[19−22] (Dexter's mechanism[23]).

* To whom correspondence should be addressed. Phone: +81-798-54-6389. Fax: +81-798-51-0914. E-mail: ykoyama@kwansei.ac.jp.
[†] Department of Chemistry, Kwansei Gakuin University.
[‡] Department of Physics, Kwansei Gakuin University.

10.1021/jp993970l CCC: $19.00
Published on Web 03/18/2000

Experimentally, time-resolved fluorescence spectroscopy using the up-conversion technique provided us with solid evidence for the involvement of the S_2 pathway, i.e., the Car-to-BChl energy transfer proceeding via the S_2 state. This was manifested by the substantially shortened lifetime of spheroidene, which is accommodated in the LH2 complex from *Rhodobactor sphaeroides* (*Rb. sphaeorides*) (~80 fs) in comparison to the lifetime of spheroidene in organic solvents (~200 fs).[5] Very recently, definitive evidence for the S_1 pathway, i.e., the S_1-state-mediated Car-to-BChl energy transfer (hereafter denoted as Car(S_1)-to-BChl(Q_y)), has been obtained by monitoring emission from B850 while exciting spheroidene directly to its S_1 state via two-photon absorption.[24] In another species, *Rps. acidophila*, the S_2 pathway was also verified by time-resolved fluorescence spectroscopy, but the involvement of the S_1 pathway has not been clear yet.[9]

In a theoretical study on the mechanisms of the Car-to-BChl energy transfer, Nagae et al.[25] proved that the S_2 state serves as an efficient donor state owing to its strong transition-dipole−transition-dipole coupling with the Q_x state of BChl (Föster's mechanism[26]); for the S_1 state, the quadrupole−dipole coupling was proved to be much more efficient than the electron-exchange coupling. Based on the crystallographic structures of the LH2 complexes, more recent theoretical analysis on *Rs. molischianum*[10] and *Rps. acidophila*[6] reached a general agreement with the view of Nagae et al.[25] However, a more detailed experimental study on the mechanism of the Car(S_1)-to-BChl(Q_y) energy transfer has been left to be attemped: In a configuration interaction (CI) calculation done by Damjanovic et al. taking into account all orders of multipoles of the S_1 state,[10] the predicted rate constant of the Car(S_1)-to-BChl(Q_y) energy transfer was about 2 orders of magnitude smaller than the experimental value. Additional mechanisms, i.e., the intensity borrowing from the S_2 state through higher vibrational levels of the S_1 state[10] as well as the break down of the C_{2h} symmetry,[25] have been proposed, both of which may speed up the Car(S_1)-to-BChl(Q_y) energy transfer. Indeed, the recent success of high-sensitivity fluorescence spectroscopy in measuring the S_1 emission of carotenoid in solution has proved that the S_1 state is weakly allowed, showing a fluorescence quantum yield as low as 10^{-6}−10^{-7}.[27,28] This partially allowed nature is proved by the resonance Raman excitation profiles probing the S_1 state of crystalline carotenoids, which could be explained by the Albrecht *A* term that is applicable to partially allowed transitions.[13,14]

The present investigation has aimed at obtaining a deeper insight into the mechanism of Car(S_1)-to-BChl(Q_y) energy transfer. To achieve this goal, we have set the following experimental strategies: (1) Th first is to determine the time constant of Car(S_1)-to-BChl(Q_y) energy transfer by means of time-resolved absorption spectroscopy. This piece of information is crucial for testing any proposition of the underlying mechanism. The rate constant of energy transfer (ps^{-1}) from a donor chromophore to an acceptor chromophore may be expressed as[29]

$$k_{ET} = 1.18|V|^2 J \qquad (1)$$

where V is the coupling (cm^{-1}) between the donor and the acceptor states and J is the overlap integral (cm) between the spectra of donor emission and acceptor absorption. One can theoretically evaluate the coupling strength ($|V|^2$) by assuming a certain mechanism, whereas J can be obtained from experimental data. The validity of a proposed mechanism relies on the extent of agreement between the theoretical and the experimental rate constants. (2) The second strategy is to obtain the fluorescence spectra of the S_1 and S_2 states in the same measurement by means of high-sensitivity steady-state fluorescence spectroscopy, from which we can obtain the following three pieces of information: (a) The overlap integral between the Car(S_1) emission and the Q_y absorptions of B800 and B850, which may allow us to make a more reliable estimation of the time constant of the Car(S_1)-to-BChl(Q_y) energy transfer. Here, it is worthwhile to mention that the Car(S_1) emission has been simply approximated by a single Gaussian distribution function with a half-width of ~3000 cm^{-1},[7,10,25] because no accurate Car(S_1) fluorescence spectra for carotenoids having more than nine conjugated C=C bonds have been available. (b) The origin of the S_1-state energy, which is crucial in discussing the mechanism of the S_1 pathway. (c) The ratio of fluorescence quantum yield between the Car(S_2) and Car(S_1) emissions. Together with the kinetic constants obtained in strategy 1, this enables us to estimate the ratio of transition dipole moments between the $S_1 \rightarrow S_0$ and $S_2 \rightarrow S_0$ emissive transitions. (3) The third strategy is to determine the molar extinction coefficients of the $S_2 \leftarrow S_0$ absorption for the relevant carotenoids in *n*-hexane. These basic parameters are essential in evaluating the transition dipole moments between the S_0 and S_2 states. (4) The fourth strategy is to examine the effect of carotenoid conjugation length on the rate and the efficiency of the S_1 pathway; this was expected to be beneficial for a general understanding of the mechanism of Car(S_1)-to-BChl(Q_y) energy transfer.

In the present investigation, we made use of the LH2 complex from *Rs. molischianum* containing a carotenoid lycopene whose number of conjugated C=C bonds, $n = 11$, and the LH2 complexes from *Rb. sphaeroides* 2.4.1 and *Rb. sphaeroides* G1C containing spheroidene ($n = 10$) and neurosporene ($n = 9$), respectively. Importantly, BChls in the LH2 complexes from these three species show the Q_y absorption at similar wavelengths, i.e., ~800 and ~850 nm, although the S_1-state energy of carotenoid increases systematically when *n* decreases.

2. Methods

Preparation of LH2 Complexes and *All-trans*-carotenoids. *Rs. molischianum* DSM 119 was cultured anaerobically at 30 °C for 3 days with a light intensity of 3000 lux in a medium modified from that of Pfennig and Trüper.[30] The cells of *Rs. molischianum* DSM 119 were disrupted at 0 °C by sonication under nitrogen atmosphere, and the chromatophores obtained were suspended in 20 mM Tris-HCl buffer (pH 8.0) at a concentration of $OD_{850} = 50\ cm^{-1}$. After being solubilized with 1% (v/v) LDAO (Fulka) for 30 min in the dark, the suspension was diluted 2-fold and centrifuged (24000*g*, 4 °C for 20 min). The supernatant was applied to sucrose density-gradient (stepwise, 0.5−2.0 M) centrifugation (200000*g*, 4 °C for 15 h) in the presence of 0.25% (w/v) sucrose monocholate. The LH2 component was purified further by using DEAE-cellulose (Whatman DE52) column chromatography in the presence of 0.1% LDAO.[31] The LH2 preparation thus obtained exhibited an A_{850}/A_{270} ratio of 2.4. The LH2 complexes from the other two species were prepared in a similar way with the following modifications: Briefly, *Rb. sphaeroides* 2.4.1 and G1C were grown in a medium containing succinate as the carbon source,[32] and the LH2 complexes were purified by DEAE-cellulose chromatography in the presence of 0.1% LDAO. The A_{850}/A_{270} ratios of the LH2 preparations were 2.7 and 2.4 for *Rb. sphaeroides* 2.4.1 and *Rb. sphaeroides* G1C, respectively.

All-trans-lycopene was extracted from tomato juice and purified following the procedure described in ref 33; *all-trans*-

TABLE 1: Pump/Probe Wavelengths, Lifetime of the S_1 State (τ_{S_1}), Time Constants (τ_{ET}), and Efficiency (η) of the Car(S_1)-to-BChl(Q_y) Energy Transfer

		n-hexane		LH2			
bacterium	carotenoid (*n*)	pump/probe (nm)	τ_{S_1} (ps)	pump/probe (nm)	τ_{S_1}[a] (ps)	τ_{ET} (ps)	η (%)
Rs. molischianum	lycopene (11)	501/554	4.7 ± 0.3	529/587	3.4 (96%)	12.3	27
Rb. sphaeroides 2.4.1	spheroidene (10)	484/529	9.3 ± 0.1	510/553	1.7 (92%)	2.1	82
Rb. sphaeroides G1C	neurosporene (9)	468/510	21.2 ± 0.1	491/535	1.3 (90%)	1.4	94

[a] Amplitudes of the exponential decay components are given in parentheses.

spheroidene and -neurosporene were isolated from the cells of *Rb. sphaeroides* 2.4.1 and *Rb. sphaeroides* G1C, respectively, and purified by using the methods described in ref 27.

Determination of the Molar Extinction Coefficients of the $S_2 \leftarrow S_0$ Absorption. *All-trans*-carotenoids, i.e., lycopene, spheroidene, and neurosporene, were crystallized twice in a mixture of *n*-hexane and tetrahydrofuran, and the extinction coefficient of each carotenoid was determined as an average of the results of two independent measurements. For each measurement, ~10.00 mg of carotenoid, weighed with an accuracy of 0.01 mg (Mettler AT201), was dissolved in 2−3 mL of tetrahydrofuran and then diluted with *n*-hexane to form a total amount of 1000 mL. This volume of solution, after ultrasonic treatment for ~10 s, served as the mother solution for the successive dilutions with factors of 2, 4, 5, and 10. The optical density was then measured for each dilution (Hitachi U-2000), and the extinction coefficient was determined by the least-squares fitting on the basis of Lambert−Beer law. HPLC analysis was performed to confirm that no sample degradation or isomerization was seen before and after each experiment.

Time-Resolved Absorption Spectroscopy. Time-resolved absorption spectroscopy was carried out for carotenoids dissolved in spectral-grade *n*-hexane (Ishizu, Ltd.) at a concentration of 8×10^{-5} M, or the LH2 complexes suspended in a buffer (20 mM Tris-HCl, pH 8.0, 0.1 LDAO%). The OD value of each LH2 preparation at a pumping wavelength was adjusted to 0.4−0.5 mm^{-1}. The sample was circulated from a sample reservior in an ice-water bath to a cell of 1 mm optical path. Pumping wavelengths, as listed in Table 1, were tuned to the zero−zero vibronic transition of the carotenoid ground-state absorption.

The pump and probe pulses were obtained as follows: A regenerative amplifier (Spectra Physics, Spitifire) seeded with a mode-locked titanium:sapphire laser (Spectra Physics, Tusnami) delivered laser pulses at 800 nm (120 fs, 1 kHz, 1 mJ/pulse), which were divided into two components by using a 10% thin-film beam splitter. The major component was sent to an optical parametric amplifier (Spectra Physics, OPA-800) generating the pump pulses (130 fs, 1 kHz, 3−8 μJ). The pumping energy was attenuated to ~0.5 μJ at the sample cell; this corresponded to a photon density of $\sim 1.2 \times 10^{14}$ photons cm^{-2}. The minor component was focused into a water cell to generate a white continuum probe. A magic-angle scheme was used in the pump−probe measurement, and the half-width of the cross-correlation traces between the pump and probe pulses were determined to be ~200 fs by the use of a nonresonant optical Kerr-effect signal. The detection system was based on a liquid-nitrogen cooled CCD (LN/CCD-1152EUV, Princeton Instruments), the details of which were described elsewhere.[33,34]

Steady-State Fluorescence Spectroscopy. Steady-state fluorescence spectroscopy was performed, at room temperature, for carotenoids dissolved in *n*-hexane purified for fluorescence measurement (Dojin Chemicals); the sample concentration was 6×10^{-6} M for each measurement. The 440 nm beam used for the excitation of neurosporene was obtained from the combination of a Xe lamp and a double monochromator (JUSCO M25D), whereas the 488 nm beam for the excitation of spheroidene and lycopene from an Ar^+ laser (NEC GLG 3050) in combination with a filter spectrometer (Spectrolab, Laser spec III). A more detailed description of the setup was given elsewhere.[27,35]

3. Results

Time Constants and Efficiencies of the Car(S_1)-to-BChl(Q_y) Energy Transfer of Carotenoids As Determined by Time-Resolved Absorption Spectroscopy. Figure 1 shows the time evolution profiles of the S_1 states for (a) lycopene, (b) spheroidene, and (c) neurosporene. In each panel, open and filled circles represent the time profiles for carotenoid dissolved in *n*-hexane and bound to LH2 complex, respectively. For each pair of profiles the probing wavelengths correspond to the maxima of the $S_n \leftarrow S_1$ spectra as listed in Table 1. After deconvolution using the instrumental response function, the decay time profiles of free and bound carotenoid could be fit by the use of single- and double-exponential functions, respectively. The time constants thus determined are summarized in Table 1. It is clearly seen, from both Figure 1 and Table 1, that the S_1 population of bound carotenoid decays faster than that of free carotenoid, evidencing the presence of Car(S_1)-to-BChl(Q_y) energy transfer. A minor long-lived component, which was necessary in fitting for each bound carotenoid, is ascribable to an excited-state species of BChl.

Assuming that the $S_1 \rightarrow S_0$ internal conversion is the only process competing with the Car(S_1)-to-BChl(Q_y) energy transfer, the rate constant, k_{ET}, and the efficiency, η, can be expressed as $k_{ET} = k - k_{IC}$ and $\eta = k_{ET}/(k_{ET} + k_{IC})$, respectively; here, k represents the decay rate constant of Car(S_1) for bound carotenoid, and k_{IC} stands for that of the $S_1 \rightarrow S_0$ internal conversion. In view of the rather weak effect of the solvent polarity and polarizability on the S_1 lifetime,[36] we assumed that the k_{IC} of a carotenoid bound to the LH2 complex is the same as that of the carotenoid dissolved in *n*-hexane. The time constant ($\tau_{ET} = k_{ET}^{-1}$) and the efficiency of the Car(S_1)-to-BChl(Q_y) energy transfer thus estimated are listed in Table 1. The results clearly demonstrate a systematic dependence of τ_{ET} on the length of the conjugated chain; i.e., τ_{ET} decreases rapidly when the number of conjugated double bonds, *n*, decreases.

Here, we note that the efficiency, η, does not refer to the efficiency in the overall Car-to-BChl energy transfer containing two pathways, but to the partition through the S_1 pathway, i.e., the energy transfer specifically originating from the Car(S_1) state. For the three LH2 complexes we examined, it seems that the efficiency of the Car(S_1)-to-BChl(Q_y) energy transfer holds close correlation to the overall efficiency; for spheroidene in *Rb. sphaeroides* 2.4.1 and neurosporene in *Rb. sphaeroides* G1C, the efficiencies via the S_1 pathway are 82 and 94% (Table 1), respectively, and then, their overall efficiencies are as high as almost unity.[37,38] For lycopene in *Rs. molischianum*, on the other hand, the efficiency via the S_1 pathway is as low as 27% (Table 1), and the overall efficiency seems less than 50%.[39]

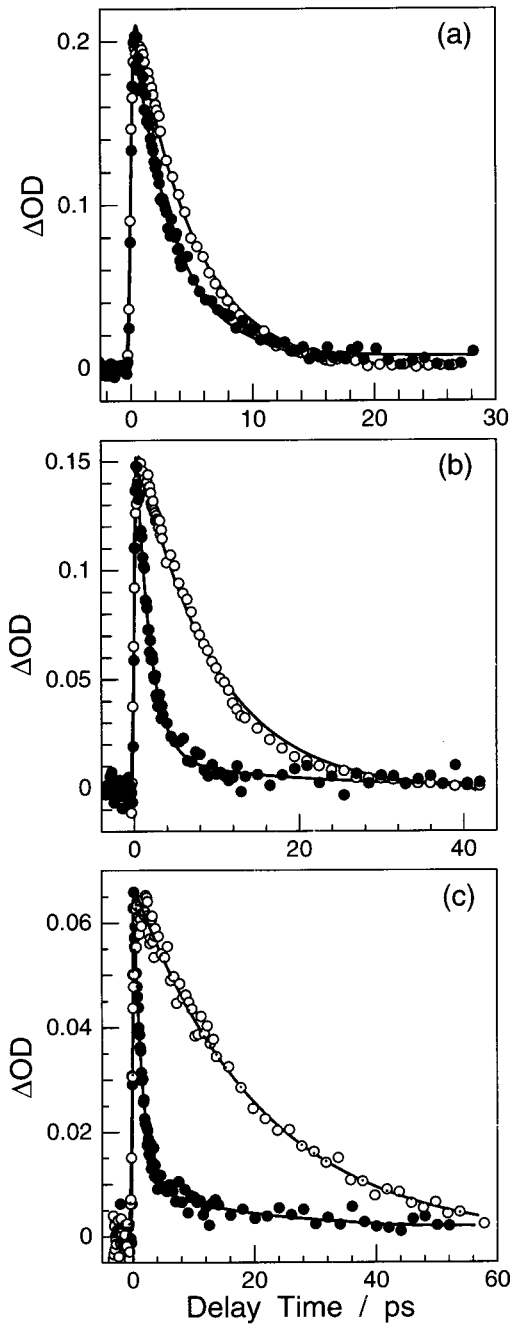

Figure 1. Time profiles of the $S_n \leftarrow S_1$ absorption for (a) lycopene, (b) spheroidene, and (c) neurosporene. Open and filled circles represent the time profiles for carotenoids free in *n*-hexane and bound to LH2, respectively. In each panel, the amplitude of a free carotenoid is normalized to that of a bound one; solid lines are the fitting curves obtained on the basis of single- or double-exponential decay functions (see text). The pump and the probe wavelengths for each trace are listed in Table 1.

S_1-State Energy and the Spectral Overlap between the Car(S_1) Emission and the Q_y Absorption of B800 and B850 for Each Carotenoid. Figure 2 illustrates the fluorescence spectra of (a) lycopene, (b) spheroidene, and (c) neurosporene in *n*-hexane. It is clearly seen that each carotenoid exhibits dual emission from both the S_1 and the S_2 states, although the intensity of the former is much weaker than the latter. In addition, upon decreasing the number of conjugated C=C bonds, the spectrum shifts systematically to the high-energy side. The origin of the S_1 state (the energy of the $S_1(0) \rightarrow S_0(0)$ transition) for each carotenoid could be determined by decomposing the

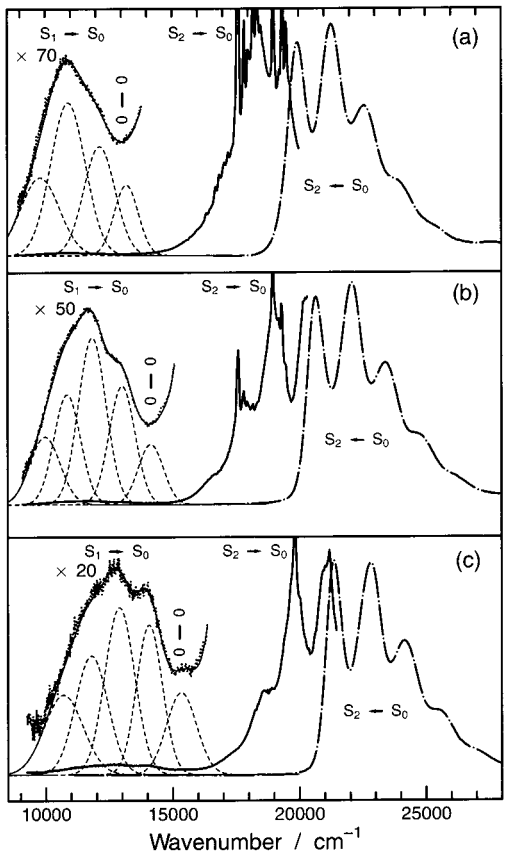

Figure 2. Fluorescence spectra recorded at room temperature for (a) lycopene, (b) spheroidene, and (c) neurosporene in *n*-hexane. In each panel, the thicker solid line shows the dual emission from the S_1 and S_2 states, the dotted line is a blow-up of the S_1 emission, and the dashed lines are the vibrational components of the S_1 emission obtained by deconvolution (those for S_2 emission are not shown for the sake of clearness), and the thinner solid line indicates the total fitting curve. The ground-state absorption spectra (dotted broken line) are also shown for reference. The sharp spectral lines on the top of the $S_2 \rightarrow S_0$ emission originate from the resonance Raman scattering.

TABLE 2: Energy Origin (E_{S_1}) of the S_1 State and Spectral Overlaps between the Car(S_1) Emission and the Q_y Absorption of B800 and B850 BChls, J_{B800} and J_{B850}

carotenoid	E_{S_1} (cm^{-1})	J_{B800} (10^{-4} cm)	J_{B850} (10^{-4} cm)
lycopene	13200 ± 90	1.776	2.163
spheroidene	14150 ± 70	2.312	3.103
neurosporene	15300 ± 80	2.405	2.071

dual emission spectrum into vibrational components having Gaussian line shapes (see Figure 2), a method which was described in ref 27. The origins of the S_1 states for the relevant carotenoids are listed in Table 2, among which the values of spheroidene and neurosporene (14 150 and 15 300 cm^{-1}) are in good agreement with those determined at 170 K (14 200 and 15 300 cm^{-1}).[27] Figure 3 presents spectra of the Car(S_1) emission (the areas are normalized) which were reconstructed by adding up the vibrational components from the Car(S_1) emission; the B800 and B850 absorptions are also shown to exhibit the spectral overlaps. It is interesting to see that the spectral overlap is delicately tuned by the energies of the vibrational structures of Car(S_1) emission; e.g., the Q_y absorption of B850 overlaps best with the $0 \rightarrow 2$ transition of spheroidene, and that of B800, with the $0 \rightarrow 2$ transition of neurosporene.

The spectral overlap can be expressed as[25]

$$J = \int_{-\infty}^{+\infty} S_D(E)\, S_A(E)\, dE \qquad (2)$$

TABLE 3: Spectral Overlaps (J) between the Car(S_1) Emission and the Q_y Absorption of Each Excitonic Level of B850 in the LH2 Complex from *Rs. molischianum* and the Time Constants (τ_{ET}) of the Car(S_1)-to-BChl(Q_y) Energy Transfer Predicted under the Monomeric and Excitonic B850 Models

monomeric B850 model			excitonic B850 model				
BChl[a]	V^b (cm^{-1})	τ_{ET} (ps)	exciton level	energy[b] (cm^{-1})	$V^{Coul\ b}$ (cm^{-1})	J (10^{-4} cm)	τ_{ET} (ps)
B850a(0)	1.29	2.35×10^3	E_1	11 482	0.537	2.267	1.14×10^4
B850b(0)	0.23	7.14×10^4	$E_{2,3}$	11 765	1.048	2.163	3.56×10^3
B850a(1)	3.79	272.17	$E_{4,5}$	12 250	1.371	1.966	2.29×10^3
B850b(1)	0.20	1.04×10^5	$E_{6,7}$	12 676	1.613	1.664	1.95×10^3
B800(0)	0.30	5.36×10^4	E_8	12 863	1.129	1.594	4.28×10^3
B800(7)	1.70	1.66×10^3	E_9	13 715	1.452	0.663	6.05×10^3
			$E_{10,11}$	13 794	1.855	0.532	4.62×10^3
			$E_{12,13}$	13 922	1.452	0.348	1.15×10^4
			$E_{14,15}$	14 012	1.048	0.246	3.13×10^4
			E_{16}	14 046	0.669	0.214	8.83×10^4
overall		210.8					372.6

[a] See Figure 4 for the labeling scheme. [b] The multipole−dipole couplings (V) for monomeric B850 and the Coulombic coupling (V^{Coul}) for excitonic B850 models, as well as the excitonic B850 energy levels, are taken from ref 10.

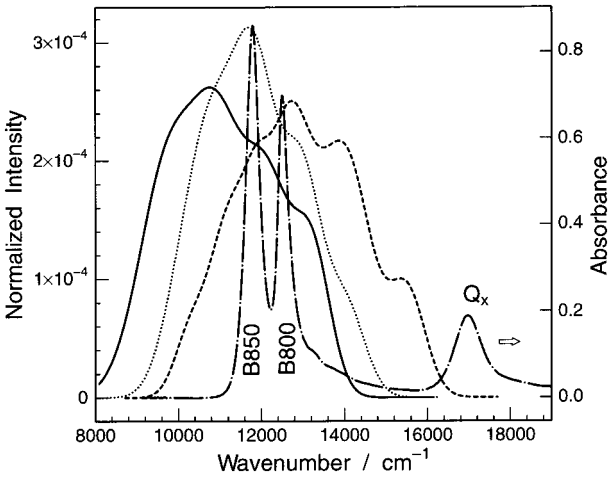

Figure 3. Reconstructed S_1-state fluorescence spectra of lycopene (solid line), spheroidene (dotted line), and neurosporene (dashed line), all of which are normalized. The ground-state absorption spectrum of the LH2 complex from *Rs. molischianum* (dotted broken line) is also shown for comparison.

where $S_D(E)$ is the spectral distribution of the S_1 emission of Car as the donor and $S_A(E)$ is that of the Q_y absorption of the B800 or B850 BChls as the acceptor; both $S_D(E)$ and $S_A(E)$ are normalized. The Car(S_1) emission determined for each carotenoid in *n*-hexane was used in evaluating the spectral overlap with the Q_y absorption of BChls in the LH2 complex; this is justified because the S_1-state energy of carotenoid is expected to be insensitive to the solvent environment.[40] Following ref 7, we approximated the B800 absorption by a Gaussian distribution which is centered at 800 nm with a homogeneous half-width of 200 cm^{-1}. The B850 absorption was treated by the use of two different models: (1) the monomeric B850 model, where the B850 absorption was assumed to have a Gaussian distribution centered at 850 nm with a homogeneous half-width of 200 cm^{-1}; (2) the excitonic B850 model, where the absorption band of the B850 BChls was regarded as a composite of a number of excitonic sublevels originating from the strong coupling among them.[41] The spectral overlaps for the monomeric B800 and B850 BChls are summarized in Table 2. For the excitonic B850 model, we adopted the excitonic sublevels in ref 10 and assumed that each of them has a Gaussian distribution with a homogeneous half-width of 200 cm^{-1}; the spectral overlaps are presented in Table 3. Note that, as a consequence of the much broader Car(S_1) emission in comparison to the B800 and B850 absorptions, an increase in the homogeneous width of the B800 and/or B850 absorptions from 200 to 300 cm^{-1} resulted in a difference of only <2% in the spectral overlap.

Time Constants of the Car(S_1)-to-BChl(Q_y) Energy Transfer Calculated by the Use of Multipole−Dipole Coupling. The S_1 to S_0 transition-dipole moment of carotenoid is supposed to vanish because of the approximate C_{2h} symmetry, as has been proved on the basis of the CI treatment of the electronic states.[10,25] However, this state has nonvanishing transition-multipole moments such as the transition-quadrupole moment. When a carotenoid molecule is brought into close proximity of a BChl molecule, as in the case of the LH2 complex, it can couple with considerable strength to the BChl molecule via the transition-multipole−transition-dipole interactions. The Car(S_1)−BChl(Q_y) coupling obtained by CI calculations has been referred to, in general, as the "Coulombic coupling" in ref 10. Since the contribution of the transition-dipole moment of Car(S_1) is negligibly small, and since the contribution of the transition-dipole moment of BChl(Q_y) is predominant over higher-order transition-miltipole moments, we would rather refer to it as "the multipole−dipole" coupling.

Using the spectral overlaps obtained in the former subsection and the Car(S_1)−BChl(Q_y) multipole-dipole couplings calculated by Damjanovic et al.[10] for lycopene in the LH2 complex of *Rs. molischianum*, we evaluated the time constant of the Car(S_1)-to-BChl(Q_y) energy transfer for both the monomeric and the excitonic B850 models; the results are summarized in Table 3. Figure 4 schematically depicts the orientation and location of the lycopene molecule and its nearby four B850 and two B800 BChl molecules in the LH2 complex from *Rs. molischianum*; the couplings between the lycopene and those BChl molecules are predominant and, hence, determine the rate of Car(S_1)-to-BChl(Q_y) energy transfer. The overall time constant predicted for the monomeric B850 model turns out to be 210.8 ps, and that for the excitonic B850 model, to be 372.6 ps; here, the channels through B800(0) and B800(7) are also taken into consideration. Both of the above time constants are much larger than the experimental value, 12.3 ps (see Table 1). On the other hand, the time constant governed by the electron-exchange coupling has been proved to be on the time scale of a few microseconds,[10,25] suggesting that this type of coupling is much less efficient in comparison to the miltipole-dipole coupling. Therefore, there must be some mechanism in operation in the Car(S_1)-to-BChl(Q_y) energy transfer besides the multipole-dipole and the electron-exchange couplings.

Transition Dipole Moment of the Car(S_1) Emission. Since the fluorescence spectrum of carotenoid in *n*-hexane exhibits weak but clear emission from the S_1 state (see Figure 2), we

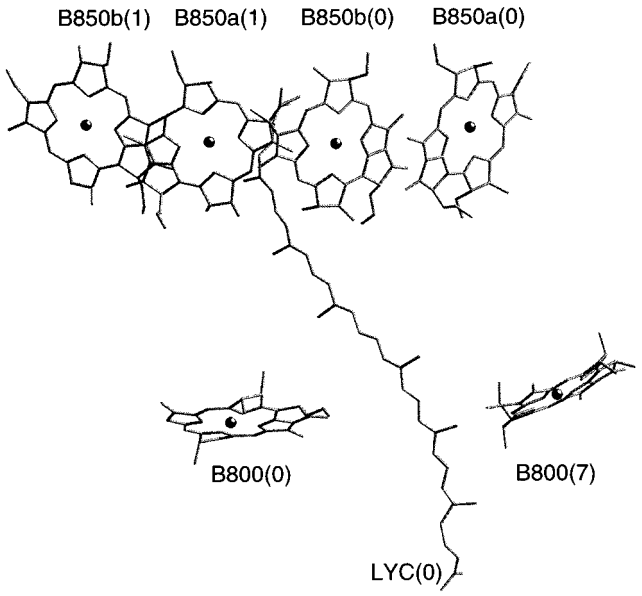

Figure 4. Schematic presentation of the lycopene (LYC) molecule and its nearby four B850 and two B800 BChls in the LH2 complex from *Rs. molischianum*. Typification of the Car and BChl molecules is also shown.

TABLE 4: Molar Extinction Coefficients (M^{-1} cm^{-1}) of the Ground-State Absorption of Carotenoids in *n*-Hexane, ϵ_{max}, in Parentheses Indicating the Value at the Absorption Maximum

transition	lycopene	spheroidene	neurosporene
$0 \leftarrow 0$	167 900	163 700	162 000 (ϵ_{max})
$1 \leftarrow 0$	181 500 (ϵ_{max})	173 600 (ϵ_{max})	159 400
$2 \leftarrow 0$	118 300	110 500	101 100
refs	185 000[a]		157 000[b]

[a] Ref 43, for the $1 \leftarrow 0$ transition. [b] Ref 44, for the $1 \leftarrow 0$ transition.

have tried to estimate the transition-dipole moment of the Car-(S_1) emission by using the fluorescence and the kinetic data which were obtained in the present study.

First, we evaluated the oscillator strength, *f*, of the S_2-S_0 transitions by using the relation[42] $f = 4.32 \times 10^{-9}\, n \int \epsilon(\tilde{\nu})\, d\tilde{\nu}$, where *n* is the refractive index of the solvent, $\tilde{\nu}$ is the frequency (cm^{-1}), and $\epsilon(\tilde{\nu})$ stands for the molar extinction coefficient of the ground-state absorption. Table 4 lists the molar extinction coefficient for each vibronic transition of each carotenoid which was determined in the present investigation; we used the ϵ_{max} value in calculating the oscillator strength. The oscillator strength divided by *n*, i.e., f_{S_2}/n, and the transition-dipole moment, μ_{S_2}, for each carotenoid are summarized in Table 5.

Second, we obtained the ratio of quantum yield ϕ_{S_1}/ϕ_{S_2} from the fluorescence spectra by taking the ratio of spectral areas of the Car(S_1) and Car(S_2) emissions; the results are also given in Table 5.

Third, we tried to determine the f_{S_1}/f_{S_2} and μ_{S_1}/μ_{S_2} ratios. For a three-level system consisting of the S_0, S_1, and S_2 states, it can be proved that the oscillator strengths, f_{S_1} and f_{S_2}, and the transition-dipole moments, μ_{S_1} and μ_{S_2}, of the Car(S_1) and Car-(S_2) emissions, hold the following relations,

$$\frac{f_{S_1}}{f_{S_2}} \approx \frac{\phi_{S_1}\tau_{S_2}E_{S_2}^{\,2}}{\phi_{S_2}\tau_{S_1}E_{S_1}^{\,2}} \tag{3}$$

$$\frac{\mu_{S_1}}{\mu_{S_2}} \approx \left(\frac{\phi_{S_1}\tau_{S_2}E_{S_2}^{\,3}}{\phi_{S_2}\tau_{S_1}E_{S_1}^{\,3}}\right)^{1/2} \tag{4}$$

where, ϕ and *E* represent the fluorescence quantum yield and the state energy respectively, each subscript indicating the relevant electronic state, and τ_{S_1} and τ_{S_2} are the time constants of the $S_1 \rightarrow S_0$ and the $S_2 \rightarrow S_1$ internal conversions, respectively. Parameters required for determining the f_{S_1}/f_{S_2} and μ_{S_1}/μ_{S_2} ratios are the following: (a) the time constants (τ_{S_1}) for carotenoids in solution listed in Table 1; (b) the time constant (τ_{S_2}) of spheroidene in *n*-pentane, ~0.25 ps, determined by time-resolved fluorescence spectroscopy,[5] and those of lycopene and neurosporene in *n*-hexane, ~0.13 and ~0.32 ps, determined by time-resolved absorption spectroscopy;[54] and (c) the state energies E_{S_1} in *n*-hexane listed in Table 2 and those E_{S_2} in *n*-hexane obtained by conventional absorption spectroscopy, i.e., 19 960, 20 660, and 21 370 cm^{-1} for lycopene, spheroidene, and neurosporene, respectively. The results are listed in Table 5. Finally, we obtained the values of f_{S_1}/n and μ_{S_1} (Table 5). Now it is clearly seen that the transition-dipole moment of the Car(S_1) emission increases systematically, when the length of the conjugated chain decreases.

4. Discussion

The results obtained in the present investigation can be summarized as follows: (1) The time constant of the Car(S_1)-to-BChl(Q_y) energy transfer (τ_{ET}) decreases systematically when the number of conjugated C=C bonds decreases. (2) In the case of *Rs. molischianum*, significant discrepancy was found between the experimentally determined time constant of the Car(S_1)-to-BChl(Q_y) energy transfer (12.3 ps) and that calculated on the basis of miltipole−dipole coupling (210.8 ps). (3) The transition-dipole moment of the Car(S_1) emission, for carotenoid in *n*-hexane, is now determined experimentally (Table 5). On the basis of these experimental results, we are now in a position to discuss the mechanism of the Car(S_1)-to-BChl(Q_y) energy transfer.

Mechanism of the Car(S_1)-to-BChl(Q_y) Energy Transfer. Between the two factors that govern the rate of energy transfer, namely, the interaction energy (*V*) and the spectral overlap (*J*) (see eq 1), we try to determine which one dominates the above conjugation-length dependence of the time constant of the Car-(S_1)-to-BChl(Q_y) energy transfer. All three carotenoids have large spectral overlaps between the Car(S_1) emission and the Q_y absorption for both the B800 and B850 BChls (see Figure 3 and Table 2); this fact implies that Car(S_1) is able to transfer energy to both B800 and B850. For lycopene, spheroidene, and neurosporene, the spectral overlaps between the Car(S_1) emission and Q_y absorption of B800 increase in the order of 1.776×10^{-4}, 2.312×10^{-4}, and 2.405×10^{-4} cm, showing only weak correlation with the order of the observed time constants of the Car(S_1)-to-BChl(Q_y) energy transfer, i.e., 12.3, 2.1, and 1.4 ps. On the other hand, the spectral overlaps between the Car(S_1) emission and the Q_y absorption of B850, i.e., 2.163×10^{-4}, 3.103×10^{-4}, and 2.071×10^{-4} cm, exhibit no direct correlation with the decreasing order of the time constants. Actually, all the above values of spectral overlaps are not too different from one another. Furthermore, we should note that the rate constant is linearly proportional to the spectral overlap, but it is proportional to the square of the electronic coupling (eq 1). Therefore, we suggest that the degree of spectral overlap should not be the dominant factor in determining the observed rapid decrease in the time constant of the Car(S_1)-to-BChl(Q_y) energy transfer when the length of the conjugated chain decreases. Thus, the dependence of the Car(S_1)-to-BChl(Q_y) energy transfer on the conjugation length must be dominated by the Car(S_1)−BChl(Q_y) coupling. This point is further

TABLE 5: Ratios of Fluorescence Quantum Yield (ϕ_{S_1}/ϕ_{S_2}), Oscillator Strength (f_{S_1}/f_{S_2}), and Transition-Dipole Moment (μ_{S_1}/μ_{S_2}) between the Car(S_1) and Car(S_2) Emissions, as Well as the Oscillator Strength[a] (f/n) and Transition-Dipole Moments (μ) of Carotenoid in *n*-Hexane

carotenoid (n)	ϕ_{S_1}/ϕ_{S_2} (%)	f_{S_1}/f_{S_2} (%)	μ_{S_1}/μ_{S_2} (%)	f_{S_2}/n	f_{S_1}/n	μ_{S_2} (D)	μ_{S_1} (D)
lycopene (11)	1.6	0.10	3.9	2.678	0.0027	16.377	0.635
spheroidene (10)	2.5	0.14	4.6	2.538	0.0036	15.646	0.720
neurosporene (9)	8.2	0.24	5.8	2.336	0.0056	14.760	0.856

[a] Where n is the refractive index of the solvent.

TABLE 6: Time Constants of the Car(S_1)-to-BChl(Q_y) Energy Transfer Predicted by the Use of Point-Dipole−Point-Dipole Approximation and CI Calculation for the LH2 Complex from *Rs. molischianum*

	point dipole−point dipole				CI[b]		
BChl[a]	separation (Å)	geometric factor	$V_{S_1-Q_y}$ (cm^{-1})	τ_{ET} (ps)	$V_{S_2-Q_y}$ (cm^{-1})	$V_{S_1-Q_y}$ (cm^{-1})	τ_{ET} (ps)
B850a(0)	15.9	−0.814	−3.98	246.6	95.16	3.71	287.5
B850b(0)	14.3	−0.168	−1.14	3.025×10^3	125.00	4.88	166.6
B850a(1)	17.1	0.913	3.57	306.6	11.86	0.46	1.851×10^4
B850b(1)	23.6	−1.797	−2.68	546.4	64.44	2.51	626.9
B800(0)	13.4	−0.556	−4.56	229.0	297.58	11.61	35.4
B800(7)	11.6	0.465	5.89	137.4	211.29	8.24	70.1
overall				47.3			18.6

[a] See Figure 4 for the labeling scheme. [b] The couplings between Car(S_2) and BChl(Q_y), $V_{S_2-Q_y}$, were taken from ref 48; the couplings between Car(S_1) and BChl(Q_y), $V_{S_1-Q_y}$, were obtained by multiplying $V_{S_2-Q_y}$ with the μ_{S_1}/μ_{S_2} ratio of 3.9% (Table 5).

supported by the following simple consideration: Taking into account only one pair of Car(S_1)−BChl(Q_y) interactions in each LH2 complexes, the couplings that are necessary to account for the experimental time constants are about 18, 36, and 50 cm^{-1} for *Rs. molischianum*, *Rb. sphaeroides* 2.4.1, and *Rb. sphaeroides* G1C, respectively. These values are about 1 order of magnitude larger than those calculated by considering the mutipole−dipole interaction (Table 3).

The aforementioned discrepancy between the experimental time constant of the Car(S_1)-to-BChl(Q_y) energy transfer and that calculated on the basis of multiople−dipole interaction implies that the multipole−dipole coupling must be much smaller than the actual coupling taking place for the carotenoids in the LH2 complexes. For instance, in the case of *Rs. molischianum*, the rate-determining, multipole−dipole coupling is 3.79 cm^{-1} (see Table 3), whereas the magnitude of "the necessary coupling" is 18 cm^{-1} as mentioned above. We have actually determined the ratios of transition-dipole moments (μ_{S_1}/μ_{S_2}), and the absolute values of μ_{S_1} for the relevant carotenoids (see Table 5). It then becomes interesting and practical to evaluate the coupling between the transition-dipole moments of the Car(S_1) emission and that of the BChl(Q_y) absorption in the LH2 complex from *Rs. molischianum*, whose structural data are available.

By using the value of the transition-dipole moment of 0.635 D for the Car(S_1) emission of lycopene (Table 5) and that of 6.132 D for the Q_y absorption of BChl,[45] we calculated the Car(S_1)−BChl(Q_y) couplings based on the point-dipole−point-dipole approximation. The couplings and the resultant time constants for the individual BChls are listed in Table 6. The overall time constant, 47.3 ps, together with the contribution of multipole−dipole interaction, 210.8 ps (Table 3), gives rise to a time constant of 38.7 ps; this value is about three times larger than the experimental value (12.3 ps). However, when the donor and acceptor molecules are in close proximity, and their separation is comparable to, or shorter than, the molecular dimensions, the point-dipole−point-dipole approximation becomes inappropriate.[8,46,47] To be more precise, we adopted the recent values of the Car(S_2)−BChl(Q_y) full Coulombic couplings which were calculated by Damjanovic et al.,[10,48] using a CI calculation, and then, estimated the Car(S_1)−BChl(Q_y) couplings by multiplying it with the μ_{S_1}/μ_{S_2} ratio of 3.9%; the overall time constants of energy transfer from lycopene to individual BChls has turned out to be 18.6 ps (Table 6); this result is in reasonable agreement with the experimental value (12.3 ps). The above results prove that our spectroscopically determined time constant of Car(S_1)-to-BChl(Q_y) energy transfer can be accounted for by scaling the Car(S_2)−BChl(Q_y) full Coulombic coupling with the ratio between the observed transition-dipole moments of the S_1 and S_2 states. The results also imply that the observed transition-dipole moment of the S_1 state may be explained by mixing the S_2 state into the S_1 state.

Possible Mechanism To Make the Carotenoid S_1 State Partially Optically Active. Given the C_{2h} symmetry of the carotenoid chromophore, whose oscillator strength associated with the S_1 to S_0 transition is supposed to vanish, it is intriguing to ask how this transition can gain such a considerably large transition-dipole moment. Extensive spectroscopic studies have demonstrated that the S_1 states of shorter *all-trans*-polyenes are fluorescent and have shown that the state mixing between the S_2 and S_1 states is responsible for emission from this "optically forbidden" state.[49] If we use the ratio of the oscillator strengths, f_{S_1}/f_{S_2}, as a measure of the degree of state mixing between the carotenoid S_1 and S_2 states, it turns out that the degree of state mixing increases in the order of lycopene ($n = 11$), spheroidene ($n = 10$), and neurosporene ($n = 9$), showing a clear dependence on the length of the conjugated chain (Table 5). Now, we will try to explore the origin of this dependence on n. We express the unperturbed wavefunctions of the S_1 and S_2 state as Ψ_{S_1} and Ψ_{S_2} and the Hamiltonian of perturbation as H' that leads to the state mixing. This perturbation can be due to instantaneous distortion of the carotenoid geometry along the non-totally-symmetric normal coordinates, or due to vibronic coupling between the S_1 and S_2 states.[50,51] We further define the perturbation energy as $K \equiv \langle \Psi_{S_2} | H' | \Psi_{S_1} \rangle$. By applying the first-order perturbation theory, it can be shown that

$$\frac{f_{S_1}}{f_{S_2}} = \frac{E_{S_1}}{E_{S_2}} \frac{K^2}{(E_{S_1} - E_{S_2})^2} \tag{5}$$

Equation 5 differs from eq 10 in ref 50 by an additional factor E_{S_1}/E_{S_2}. For a shorter polyene such as diphenyloctatetraene, $E_{S_1}/E_{S_2} = 0.9$, but for a carotenoid having a longer conjugated chain

such as β-carotene, E_{S_1}/E_{S_2} becomes as low as 0.7; therefore, this factor must be taken into account for the present carotenoids. Using eq 5 and the experimental values of f_{S_1}/f_{S_2}, E_{S_1}, and E_{S_2}, we estimated the perturbation energies (K) for lycopene, spheroidene, and neurosporene to be 263, 294, and 351 cm^{-1}, respectively. Most importantly, eq 5 predicts that the degree of state mixing is inversely proportional to the square of the energy gap, $E_{S_1} - E_{S_2}$. This relation is supported by the experimental observation; i.e., when the energy gap between S_1 and S_2 states decreases in the order of lycopene (6760 cm^{-1}), spheroidene (6510 cm^{-1}), and neurosporene (6070 cm^{-1}), the f_{S_1}/f_{S_2} value increases in the order of 0.10, 0.14, and 0.24%, respectively. Thus, we have shown that the state mixing between the S_1 and S_2 states is a major factor in determining the relative oscillator strengths of the S_1 emission from the relevant carotenoids.

Car(S_1)-to-BChl(Q_y) Energy Transfer for Spheroidene and Neurosporene in the LH2 Complexes. For lycopene in the LH2 complex of *Rs. molischianum*, the present study has shown that the Car(S_1)-to-BChl(Q_y) energy transfer can be explained in terms of the state mixing between S_2 and S_1 states and by invoking the Car(S_2)-to-BChl(Q_y) full Coulombic coupling scaled by a ratio of the state mixing. Does the same mechanism hold true for the LH2 complex from the other two species, *Rb. sphaeroides* 2.4.1 and *Rb. sphaeroides* G1C? Unfortunately, we cannot draw any conclusion due to the absence of structural information on those LH2 complexes. However, if we assume that the geometric factors concerning the Car and BChl molecules were the same, the time constants of Car(S_1)-to-BChl(Q_y) energy transfer, estimated by the use of μ_{S_1} values in Table 5 and of the point-dipole−point-dipole approximation, turns out to be 24.0 and 20.0 ps for spheroidene ($n = 10$) and neurosporene ($n = 9$), respectively. In comparison to the time constant for lycopene ($n = 11$) determined by the same method (38.7 ps), the calculated time constant does decrease when n decreases, in agreement with the trend of observed time constant (τ_{ET}), but the latter decreases more rapidly (see Table 1). Spectroscopic data exhibit similarity between the LH2 complexes from *Rs. molischianum* and *Rb. sphaeroides*, suggesting that the structural motif is the same, but they are different in the size of the B850 ring; the former contains eight repeating subunits, whereas the latter, six subunits.[52] Furthermore, the orientation of the carotenoid and BChl molecules is likely to be species dependent.[52,53] It is expected that, for closely packed carotenoid and BChl molecules in the LH2 complexes, even slight variation in separation and/or in relative orientation between the Car and BChl molecules can considerably alter the coupling strength. Therefore, the structural information on the LH2 complexes from *Rb. sphaeroides* 2.4.1 and G1C is absolutely necessary for elucidating the mechanism of the Car(S_1)-to-BChl(Q_y) energy transfer in those organisms. We also need to examine the mechanism of Car(S_2)-to-BChl(Q_x) energy transfer in more detail to elucidate the singlet energy-transfer processes in total. The possible involvement of the newly identified $1B_u^-$ state in the $1B_u^+$-to-$2A_g^-$ internal conversion may cause further complication in the total energy-transfer processes.[13,14]

5. Conclusions

The results of time-resolved absorption spectroscopy presented in this study have revealed a systematic dependence of the time constant of the Car(S_1)-to-BChl(Q_y) energy transfer on the conjugation length of carotenoids in the LH2 complexes from *Rs. molischianum*, *Rb. sphaeroides* 2.4.1, and *Rb. sphaeroides* G1C. The results of steady-state fluorescence spectroscopy, together with the above results of time-resolved absorption spectroscopy, allowed us to estimate the magnitudes of transition-dipole moments associated with the Car(S_1) emission for lycopene, spheroidene, and neurosporene in *n*-hexane. In the case of *Rs. molischianum*, whose structural information on the LH2 complex is now available, the value of the time constant of the Car(S_1)-to-BChl(Q_y) energy transfer, predicted by using the Car(S_2)-to-BChl(Q_y) full Coulombic coupling that is scaled by a ratio of the state mixing, is in reasonable agreement with the experimental value. Furthermore, we have proposed that the oscillator strength of Car(S_1) emission, showing clear conjugation dependence, originates from the state mixing between the carotenoid S_2 and S_1 states. The present results have provided a new piece of information concerning the Car-to-BChl energy transfer to be examined further by theoretical studies. In particular, the excitonic nature of B850 BChls in the LH2 complexes must be taken into account in more detail. In addition, the detailed mechanism of the state mixing should be revealed by further experimental and theoretical studies.

Acknowledgment. The authors would like to thank Ana Damjanovic and Prof. Klaus Schulten for sharing the results of ref 48; they are also indebted to Dr. Brent P. Krueger for reading the manuscript in its preliminary stage and for making helpful suggestions. We are grateful to Prof. Hugo Scheer for providing us the strain of *Rs. molischianum*, and to Kazukimi Hara, Yuki Sadakage and Kentaro Furuichi for their assistance in determining the molar extinction coefficients. This work has been supported by a grant from the Science Research Promotion Fund and by a grant from the Japan Society for the Promotion of Science.

References and Notes

(1) Frank, H. A.; Cogdell, R. J. *Photochem. Photobiol.* **1996**, *63*, 257.
(2) Koyama, Y.; Kuki, M.; Andersson, P. O.; Gillbro, T. *Photochem. Photobiol.* **1996**, *63*, 243.
(3) McDermott, G.; Prince, S. M.; Freer, A. A.; Hawthornthwaite-Lawless, A. M.; Papiz, M. Z.; Cogdell, R. J.; Isaacs, N. W. *Nature* **1995**, *374*, 517.
(4) Koepke, J.; Hu, X.; Muenke, C.; Schulten, K.; Michel H. *Structure* **1996**, *4* (5), 581.
(5) Ricci, M.; Bradforth, S. E.; Jimenez, R.; Fleming, G. R. *Chem. Phys. Lett.* **1996**, *259*, 381.
(6) Scholes, G. D.; Harcourt, R. D.; Fleming, G. R. *J. Phys. Chem. B* **1997**, *101*, 7302.
(7) Krueger, B. P.; Scholes, G. D.; Jimenez, R.; Fleming, G. R. *J. Phys. Chem. B* **1998**, *102*, 2284.
(8) Krueger, B. P.; Scholes, G. D.; Fleming, G. R. *J. Phys. Chem. B* **1998**, *102*, 5378.
(9) Macpherson, A. N.; Arellano, B.; Fraser, N.; Cogdell, R. J.; Gillbro, T. In *Photosynthesis: Mechanism and Effects*, Vol. I; Garab, G., Ed.; Kluwer Academic Publishers: Dordrecht, The Netherlands, 1998; p 9.
(10) Damjanovic, A.; Ritz, T.; Schulten, K. *Phys. Rev. E* **1999**, *59*, 3293.
(11) Sundström, V.; Pullerits, T.; van Grondelle, R. *J. Phys. Chem. B* **1999**, *103*, 2327.
(12) Desamero, R. Z. B.; Chynwat, V.; van der Hoef, I.; Jansen, F. J.; Lugtenburg, J.; Gosztola, D.; Wasielewski, M. R.; Cua, A.; Bocian, D. F.; Frank, H. A. *J. Phys. Chem. B* **1998**, *102*, 8151.
(13) Sashima, T.; Nagae, H.; Kuki, M.; Koyama, Y. *Chem. Phys. Lett.* **1999**, *299*, 187.
(14) Sashima, T.; Koyama, Y.; Yamada, T.; Hashimoto, H. *J. Phys. Chem. B.* submitted for publication.
(15) Song, P.-S.; Moore, T. A. *Photochem. Photobiol.* **1974**, *19*, 435.
(16) Gillbro, T.; Cogdell, R. J. *Chem. Phys. Lett.* **1989**, *158*, 312.
(17) Shreve, A. P.; Trautman, J. K.; Frank, H. A.; Owens, T. G.; Albrecht, A. C. *Biochim. Biophys. Acta* **1991**, *1058*, 280.
(18) Kandori, H.; Sasabe, H.; Mimuro, M. *J. Am. Chem. Soc.* **1994**, *116*, 2671.
(19) Naqvi, K. R. *Photochem. Photobiol.* **1980**, *31*, 523.
(20) van Grondelle, R. *Biochim. Biophys. Acta* **1985**, *811*, 147.
(21) Siefermann-Harms, D. *Biochim. Biophys. Acta* **1985**, *811*, 325.
(22) Cogdell, R. J.; Frank, H. A. *Biochim. Biophys. Acta* **1987**, *895*, 63.

(23) Dexter, D. L. *J. Chem. Phys*. **1953**, *21*, 836.
(24) Krueger, B. P.; Yom, J.; Walla, P. J.; Fleming, G. R. *Chem. Phys. Lett.* **1999**, *310*, 57.
(25) Nagae, H.; Kakitani, T.; Katoh, T.; Mimuro, M. *J. Chem. Phys.* **1993**, *98*, 8012.
(26) Föster, Th. In *Modern Quantum Chemistry*, Vol. III; Academic Press: New York, 1965; p 93.
(27) Fujii, R.; Onaka, K.; Kuki, M.; Koyama, Y.; Watanabe, Y. *Chem. Phys. Lett*. **1998**, *288*, 847.
(28) Fujii, R.; Onaka, K.; Nagae, H.; Koyama, Y.; Watanabe, Y. *J. Lumin.*, submitted for publication.
(29) Pullerits, T.; Hess, S.; Herek, J. L.; Sundström, V. *J. Phys. Chem. B* **1997**, *101*, 10560.
(30) Pfennig, N.; Trüper, H. G. *Int. J. Syst. Bacteriol*. **1971**, *21*, 19.
(31) Feher, G.; Okumura, M. Y. In *The Photosynthetic Bacteria*; Clayton, R. K., Sistrom, W. R., Eds.; Plenum Press: New York, 1978; p 349.
(32) Bose, S. K. In *Bacterial Photosynthesis*; Gest, H., Pietro, A. S., Vernon, L. F., Eds.; Antioch Press: Yellow Springs, OH, 1963; p 501.
(33) Zhang, J.-P.; Chen, C.-H.; Koyama, Y.; Nagae, H. *J. Phys. Chem. B* **1998**, *102*, 1632.
(34) Limantara, L.; Fujii, R.; Zhang, J.-P.; Kakuno, T.; Hara, H.; Kawamori, A.; Yagura, T.; Cogdell, R. J.; Koyama, Y. *Biochemistry* **1998**, *37*, 17469.
(35) Miki, Y.; Kameyama, T.; Koyama, Y.; Watanabe, Y. *J. Phys. Chem.* **1993**, *97*, 6142.
(36) Frank, H. A.; Bautista, J. A.; Gosztola, D.; Wasielewski, M. R. In *Photosynthesis: Mechanism and Effects*, Vol. I; Garab, G., Ed.; Kluwer Academic Publishers: Dordrecht, The Netherlands, 1998; p 473.
(37) Cogdell, R. J.; Hipkins, M. F.; MacDonald, W.; Truscott, T. G. *Biochim. Biophys. Acta* **1981**, *634*, 191.
(38) van Grondelle, R.; Kramer, H. J. M.; Rijgersberg, C. P. *Biochim. Biophys. Acta* **1982**, *682*, 208.
(39) Frank, H. A.; Cogdell, R. J. In *Carotenoids in Photosynthesis*; Young, A., Britton, G., Eds.; Chapman & Hall: London, 1993; p 252.
(40) Andersson, P. O.; Gillbro, T.; Ferguson, L.; Cogdell, R. J. *Photochem. Photobiol.* **1991**, *54*, 353.
(41) Hu, X.; Ritz, T.; Damjanovic, A.; Schulten, K. *J. Phys. Chem. B* **1997**, *101*, 3854.
(42) Mataga, N.; Kubota, Y. *Molecular Interaction and Electronic Spectra*; Marcel Dekker, Inc.: New York, 1970; Chapter 3.
(43) Zechmeister, L. *Cis*−*Trans Isomeric Carotenoids and Arylpolyenes*; Academic Press Inc. Publishers: New York, 1962; p 29.
(44) Britton, G. In *Carotenoids*, Vol. 1B; Britton, G., Liaaen-Jensen, S., Pfander, H., Eds.; Birkhauser Verlag: Basel, Switzerland, 1995; p 13.
(45) Sauer, K.; Lindsay Smith, J. R.; Schultz, A. J. *J. Am. Chem. Soc*. **1966**, *88*, 2681.
(46) Chang, J. C. *J. Chem. Phys*. **1977**, *67*, 3901.
(47) Scholes, G. D.; Gould, I. R.; Cogdell, R. J.; Fleming, G. R. *J. Phys. Chem. B* **1999**, *103*, 2543.
(48) Damjanovic, A.; Schulten, K. Unpublished results.
(49) Hudson, B. S.; Kohler, B. E.; Schulten, K. In *Excited States*, Vol. 9; Lim, E. C., Ed.; Academic Press: New York, 1982; p 1.
(50) Hudson, B. S.; Kohler, B. E. *J. Chem. Phys.* **1973**, *59*, 4984.
(51) Andrews, J. R.; Hudson, B. S. *J. Chem. Phys.* **1978**, *68*, 4587.
(52) Beekman, L. M. P.; Frese, R. N.; Fowler, G. J. S.; Picorel, R.; Cogdell, R. J.; van Stokkum, I. H. M.; Hunter, C. N.; van Grondelle, R. *J. Phys. Chem. B* **1997**, *101*, 7293.
(53) Koolhaas, M. H. C.; Frese, R. N.; Fowler, G. J. S.; Bibby, T. S.; Georgakopoulou, S.; van der Zwan, G.: Hunter, C. N.; van Grondelle, R. *Biochemistry* **1998**, *37*, 4693.
(54) Zhang, J.-P.; Inaba, T.; Koyama, Y. Unpublished results.